Volume 1 | Number 1 | Jan 2013 | Pages 1–100

Nanoscale

www.rsc.org/nanoscale

ROYAL SOCIETY OF CHEMISTRY

ROYAL SOCIETY OF CHEMISTRY

www.rsc.org/nanoscale

Journal Name

Aligned Platinum Nanowire Networks from Surface-Oriented Lipid Cubic Phase Templates

S.J. Richardson[a], M.R. Burton[b], P.A. Staniec[c], I.S. Nandhakumar[b], N.J. Terrill[c], J.M. Elliott[a], A.M. Squires[a]*

Mesoporous metal structures featuring a bicontinuous cubic morphology have a wide range of potential applications and novel opto-electronic properties, often orientation-dependent. We describe the production of nanostructured metal films 1-2 microns thick featuring 3D-periodic 'single diamond' morphology that show high out-of-plane alignment, with the (111) plane oriented parallel to the substrate. These are produced by electrodeposition of platinum through a lipid cubic phase (Q_{II}) template. Further investigation into the mechanism for the orientation revealed the surprising result that the Q_{II} template, which is tens of microns thick, is polydomain with no overall orientation. When thicker platinum films are grown, they also show increased orientational disorder. These results suggest that polydomain Q_{II} samples display a region of uniaxial orientation at the lipid/substrate interface up to approximately 2.8 ± 0.3 μm away from the solid surface. Our approach gives previously unavailable information on the arrangement of cubic phases at solid interfaces, which is important for many applications of Q_{II} phases. Most significantly, we have produced a previously unreported class of oriented nanomaterial, with potential applications including metamaterials and lithographic masks.

Introduction

Mesoporous materials have wide-reaching applications in the field of nanotechnology; the ordered nature of these structures has led to uses within lithography[1], catalysis[2–4], drug delivery[5], molecular sieves[6], batteries[7], sensors[8] and solar cells[9]. Bicontinuous cubic structures such as the gyroid are particularly advantageous due to their 3D morphology which allows for enhanced diffusion[10] and electron transport[11] in addition to high mechanical stability[11,12] and catalytic durability[3,4,13]. Typically these materials are fabricated in the gyroid form using a corresponding surfactant ordered silica[3,11,14] or etched block copolymer[4,15] template. (These examples were all used to produce gyroidal 3D platinum nanowire networks). However it has also been demonstrated that metals can be templated directly from lyotropic liquid crystal structures.[16,17] Direct liquid crystal templating from type I and II systems has been shown to be a facile, chemically green and cheap method to produce well-ordered nanostructures with a variety of morphologies[17] and we have recently shown that this can be extended to bicontinuous cubic lipid systems[18]. The procedure, including template formation and subsequent removal, takes approximately an hour, as

compared with over a week for block copolymer[4] or silica[3] templating routes, and does not require harsh chemical or environmental conditions for template removal.

Type II lipids form three different bicontinuous cubic phases; in addition to the gyroid ($Q_{II}{}^G$) they can also form the 'primitive' ($Q_{II}{}^P$) and 'double diamond' ($Q_{II}{}^D$). All three feature a continuous lipid bilayer formed around two discreet water channel networks. We demonstrated templated electrodeposition of platinum through the $Q_{II}{}^D$ phase of the lipid phytantriol[18], exploiting the fact that type II lipids can form the $Q_{II}{}^D$ phase in excess water conditions[19] which allowed the template to be applied as a thin film. Platinum deposition was found to occur only in a single water network, which was considered to arise from capping of one of the channels at the cubic phase surface; the resulting structure featured a 'single diamond' morphology with Fd3m symmetry, in contrast to the Pn3m symmetry of the 'double diamond' lipid template. These films were well ordered as demonstrated by small angle X-ray scattering (SAXS) data but still polydomain, giving 'powder-like' scattering patterns comprising sharp Debye-Scherrer rings.

Typically the properties of materials are enhanced by producing 'single-crystal' like single domain structures[20] and it has been predicted that this should result in an enhancement in transport as well as mechanical properties[21]. Orientation is also important for periodic nanostructures used as lithographic masks where the nanoscale pores allow for higher feature density than possible with conventional lithography[1,22]. Additionally, gold structures with a uniaxial aligned gyroid morphology have been demonstrated to function as metamaterials for visible light, featuring exotic optical properties that depend on nanostructure orientation[23,24]. However, no oriented metal nanomaterials with any other bicontinuous cubic morphology have been produced.

a. Department of Chemistry, University of Reading, Whiteknights, Reading, RG6 6AD, UK
b. Department of Chemistry, University of Southampton, University Road, Southampton SO17 1BJ, UK
c. Diamond Light Source Ltd, Diamond House, Harwell Science and Innovation Campus, Didcot, OX11 0DE, UK
* Corresponding Author: a.m.squires@reading.ac.uk

There have been several reported methods of how to produce a Q_{II} phase with an overall alignment by constraining sample dimensions[25–27], controlled hydration[20] and by shear flow[28–30].While it might be expected that in order to template an orientated metal structure the lipid template must also feature an overall alignment, we demonstrate in this paper that it is possible to produce an orientated metal nanostructure using a polydomain lipid template with no overall orientation.

By depositing our templated platinum structures onto thin gold foil which can be measured in both perpendicular and parallel configuration to the SAXS beam we are able to collect both in-plane (defined as plane parallel to the substrate) and out-of-plane (plane perpendicular to the substrate) data which typically requires both transmission SAXS and grazing incidence (GISAXS) or reflection SAXS measurements[25,27,31,32]. Through this technique, we demonstrate that we can reproducibly fabricate platinum nanostructures with an Fd3m morphology aligned with the (111) plane parallel to the substrate.

The crystallographic symmetry of the platinum film (Fd3m) is different to that of the lipid templates (Pn3m) which gives rise to additional reflections that are absent in Pn3m. Due to this difference in symmetries, it was possible to obtain a scattering signal from the orientated platinum film in the presence of the polydomain Q_{II} template before removal of the lipid. These measurements demonstrated that the orientated platinum nanostructures were produced from polydomain Q_{II} phase templates that had no overall orientation. This suggests that, while the lipid template is on average polydomain, a region of the lipid close to the electrode remains orientated with the (111) planes aligned parallel to the substrate. This is supported by previous theoretical work based on bilayer curvature which has shown that the observed orientation is most favourable for a Q_{II} phase at an interface, with a closed bilayer[26]. Previously, measurements of the lipid surface at the lipid/water interface have been made using atomic force microscopy[33] but no comparable information on the lipid/substrate interface has been obtained. This has implications for electrodes modified by Q_{II} phases[34] and is important information for others producing templated materials from lipid cubic phases as it will dictate the structure of the templated material at the substrate.

Experimental

All chemicals were used as received. Phytantriol (3,7,11,15-tetramethyl-1,2,3-hexadecanetriol, purity > 98.3 %) was purchased from Adina Cosmetics; chloroplatinic acid (dihydrogen hexachloroplatinate(2–)) solution (8% w/w in water) was purchased from Sigma-Aldrich.

Nanostructured platinum films were deposited through films of dip coated phytantriol in a fashion similar to that previously reported by Akbar[18]. Deposition was carried out on gold foil substrates (5 mm × 12.5 µm × 0.5 mm) which were initially cleaned through cycling in 0.5 M H_2SO_4 at 0.2 V/s between -0.2 and 1.8 V vs. Ag/AgCl until the cyclic voltammogram remained steady. The lipid template was applied by dip coating in a solution of ethanol and 30% or 60% (w/w) phytantriol. Once the template was applied, the substrates were left for 30 minutes in air in order for the ethanol to evaporate, leaving a thin film of phytantriol on the substrate surface, estimated

by weight to be 16 ± 0.3 µm in thickness for solutions of 30% phytantriol[35] and 22 ± 1 µm for solutions of 60% phytantriol. Platinum was deposited in a conventional three electrode electrochemical cell using the lipid coated substrate as the working electrode, a 1 cm^2 platinum mesh as a counter and a Ag/AgCl reference electrode. All three electrodes were held vertically, with the foil substrate working electrode edge on to the counter electrode in order to minimise differences in conditions on either side of the foil. Before deposition the lipid coated substrate was allowed to soak for 10 minutes to allow the lipid to hydrate, forming a Q_{II}^D phase on the surface. Platinum was deposited at a potential of -0.25 V vs. Ag/AgCl for either 300 s, 600 s or 900 s. After deposition platinum and lipid coated substrates were washed in Milli-Q water before being submerged in ethanol for 30 minutes in order to remove the lipid template. After soaking, the electrodes were removed and washed again in ultra-pure water leaving a nanostructured platinum film on the gold substrate. The timings for the various steps in Q_{II} template formation and removal were chosen following our published protocols[18]; the procedure has been thoroughly characterised[35].

SAXS measurements were performed at beamline I07 at Diamond Light Source, I911-SAXS at Maxlab and BM28 - XMaS at ESRF, respectively using beam energies of 13 keV, 13.6 keV and 15 keV and beam dimensions 200 µm x 200 µm, 300 µm x 300 µm and 250 µm x 250 µm. A Pilatus 2M, Pilatus 1M and MAR165 detectors were used to collect data over a range of 0.01 – 0.3 Å at Diamond, Maxlab and ESRF respectively. A sample of silver behenate was used as a calibrant in order to measure the sample to detector distance and determine the beam centre in each case. Deposited platinum films were measured perpendicular (face on) and parallel (edge on) to the beam in order to measure the in-plane and out-of-plane orientation respectively. Measurements of lipid coated gold films were taken before any platinum deposition as well as platinum/lipid films which were quickly submerged in water after deposition. Lipid coated gold foil and platinum/lipid films were held in a custom 3D-printed water cell with Kapton windows to allow X-ray transmission. The cell was made with a path length of 7 mm which was short enough to allow for SAXS data to be obtained.

Two-dimensional SAXS images were radially and azimuthally integrated using YAX[36,37], a custom macro that runs within the ImageJ software package. Phases were identified by assigning peaks measured to Bragg reflections for a given phase. Simulated spot patterns were produced using previously published calculations[25,27] as detailed in S1.

Scanning electron microscope (SEM) images were taken using an FEI Quanta FEG 600 environmental scanning electron microscope. Platinum coated foil samples were mounted side on onto adhesive carbon discs, see S5. Transmission electron microscope (TEM) images were taken of phytantriol-directed platinum. A film was deposited for 300 s and then scraped off the gold foil substrate with a scalpel. The resulting platinum powder was pressed onto a Lacey Carbon film on Copper 300 mesh and investigated using a using a Philips CM20 Analytical TEM. Electrochemical characterisation of sample surface area was performed on platinum films deposited onto custom gold disc electrodes (d = 0.5mm). Samples were cycled in 0.5M H_2SO_4 between -0.3 and 1.2 V vs. Ag/AgCl.

Results and discussion

Platinum nanostructures templated using the Q_{II} phase formed by phytantriol at excess hydration were deposited onto gold foil; models of both the template and deposited platinum structure are shown in Fig. 1.
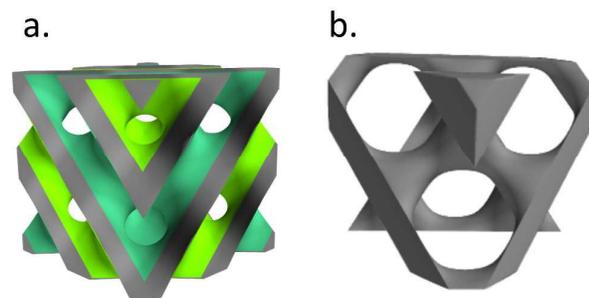

Figure 1. (a) Q_{II}^{D} 'double diamond' phase where grey region is occupied by lipid bilayer, (b) corresponding 'Single diamond' platinum structure.

In order to describe the position of the sample with respect to the beam, an experimental axis relative to the sample was defined. Schematics for the two measurement configurations (xy and zy, obtained with beam travelling in the z and x directions respectively) are shown in Fig. 2, along with corresponding SAXS patterns of a phytantriol directed platinum nanostructure. In Fig. 2c a ring is observed indicating no overall orientation in the xy plane. In Fig. 2d, spots are observed which indicates a high degree of orientation of the platinum structure in the zy plane. These images clearly demonstrate that the platinum structure displays uniaxial orientation, i.e. fibre averaged about an axis perpendicular to the electrode surface. The scattering pattern produced by the orientated structure closely matches the predicted scattering pattern for Fd3m symmetry orientated with the (111) plane (a/d = √3) parallel to the substrate which has been superimposed onto Fig. 2d. An offset angle has been added to the simulated pattern to account for offset of the foil sample determined from the horizontal scatter from the foil substrate. The on axis reflections are observed to be more intense which is predicted by the Lorentz factor for uniaxial orientation.[29,38] The √8 and √12 reflections are difficult to see on the same image as the √3 reflections due to contrast difference; an adjusted image showing the outer reflections is shown in S2 where again the positions match predictions. Interestingly, the lattice has undergone a slight tetragonal elongation in the z direction, with lattice parameters a=b=140 ± 1 Å and c= 150.3 ± 0.1 Å (see S3) where a,b,c are the unit cell dimensions in the x,y,z directions respectively. This result is in contrast to previous observations on double gyroid structures produced using a silica template where a contraction in the z direction was observed after template removal[3]. Under the conditions listed four samples were fabricated each producing similar scattering patterns demonstrating the reproducibly of this work. This is the first report of the production of an oriented metal nanomaterial with single diamond morphology (Fd3m symmetry).
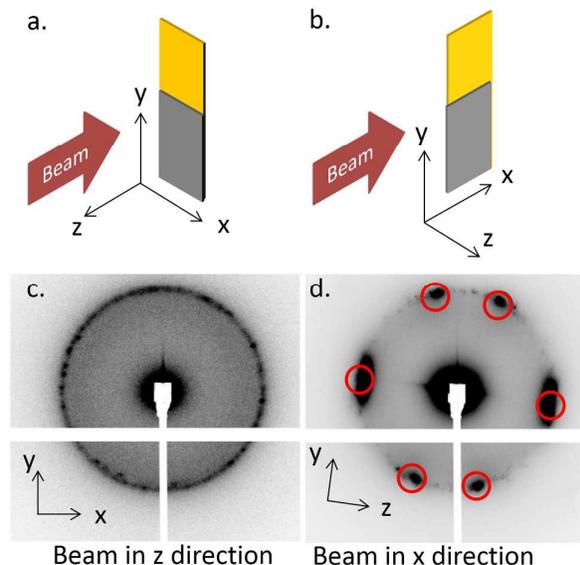

Figure 2. Schematic of in-plane and out-of-plane measurements (a – b) with representative images of nanostructured platinum film measured in each configuration (c-d). Predicted scattering pattern for a structure with a Fd3m morphology with the (111) plane orientated parallel to the substrate has been superimposed as circles on image (d).

SEM images of the foils were taken in order to investigate the homogeneity of the films as well as to measure the thickness. Fig. 3 shows an SEM image of a nanostructured platinum film on a piece of gold foil. The image was taken from the side of the foil in the configuration as shown in S5 along with additional SEM images. Chemical analysis performed by EDX confirmed that the lower area was the gold substrate and the deposit on top is the platinum film. In general, the platinum films show good adherence to the substrates. In some places, the platinum film was seen to flake off; this is not surprising given the flexible nature of the gold foil substrate, and the fact that the samples had undergone a lot of bending and flexing during x-ray analysis and transportation to and from synchrotron facilities before the SEM images were obtained. Flaking of the platinum allowed us to obtain SEM images showing film thickness, see S5. A TEM image of the deposited platinum nanostructure is shown in Fig 4. A porous network of nanowires can be clearly observed. A more detailed characterisation of the unoriented material is contained in the reference by Akbar et al.[18] where TEM images confirm the 3D network of nanowires 2-3nm in diameter. The sample surface area was measured electrochemically and determined to be 44 ± 1 m2/g, further indicating a mesoporous structure (see S4).

Nanoscale Accepted Manuscript
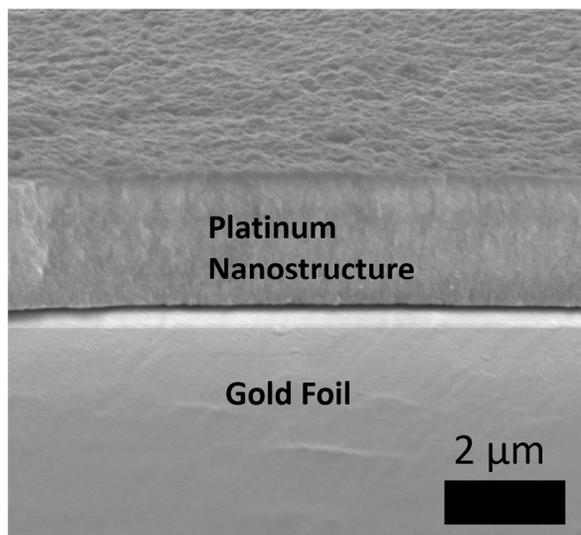
Figure 3. SEM image of a platinum nanostructure deposited onto a gold foil substrate. Image was captured in the zy plane with EDX used to confirm platinum and gold regions.

In the remainder of this manuscript we study the mechanism for the observed alignment. Previously we have studied lipid films produced by spin coating and found they too were orientated with the (111) plane parallel to the substrate which we suggested was due to minimisation of interfacial energy due to constrained sample dimensions[27]. However the dip coated phytantriol films used to direct platinum deposition are far thicker than the films produced by spin coating (16 µm vs. 1 µm) so cannot be assumed to adopt the same orientation. In order to investigate these dip coated films we obtained a SAXS pattern in the zy plane of a gold substrate, dip-coated in phytantriol and the immersed in water as shown in Fig. 4. A custom liquid-SAXS cell was built in order to facilitate this measurement. No clear orientation of the lipid film can be observed; orientated samples display a regular spot pattern[28,29] which is not observed here. Instead a randomly-orientated polydomain sample is demonstrated by the presence of Debye-Scherrer rings with uniform intensity (azimuthal profiles of inner reflection shown in supporting information Fig. S5a). The radial profile (Fig. S5b) shows that the sample has formed a saturated Q_{II}^{D} phase with the lattice parameter of a = 69.2 ± 0.1 Å which agrees with previous measurements[19] and is approximately half of the single diamond structure due to differences in symmetry[18].
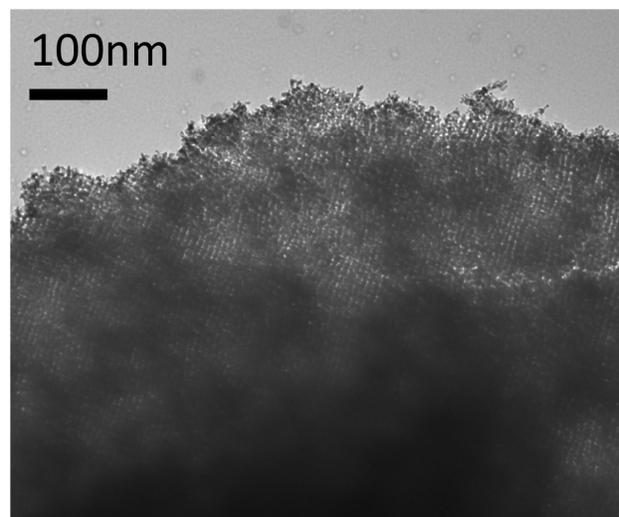

Figure 4. TEM image of platinum deposit.
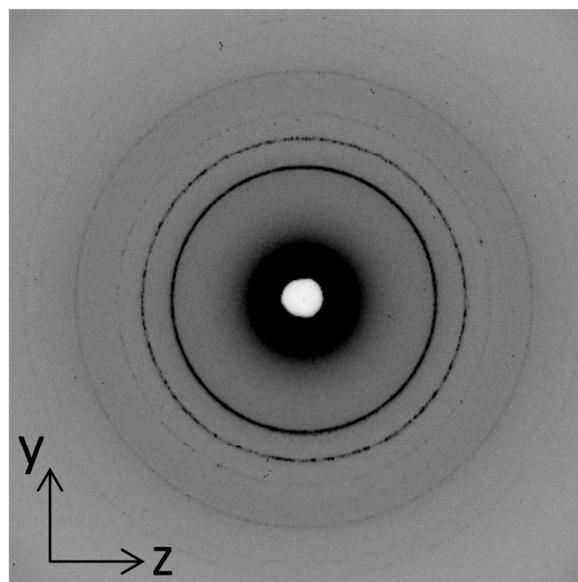
Figure 5. SAXS image taken in the zy plane of a thin lipid film on gold foil substrate dip coated from ethanol and 30% phytantriol solution displaying Q_{II}^{D} phase.

Furthermore, it was possible to simultaneously investigate both the platinum and the template; as the platinum nanostructures are only observed to deposit in a single water channel of the Q_{II} phase[18] differing structural symmetries are observable by SAXS for the
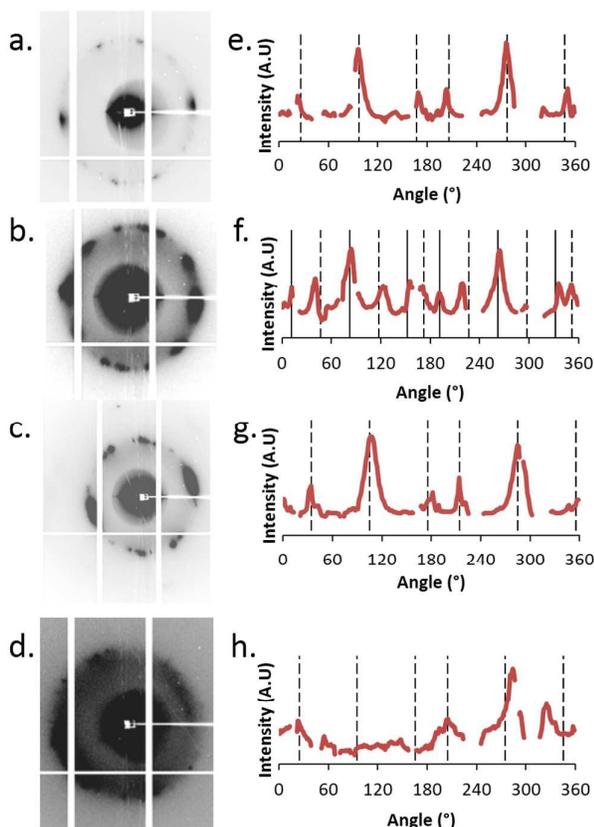
platinum (Fd3m) and lipid structures (Pn3m), giving unique reflections for Fd3m that are systematic absences for Pn3m. SAXS images were taken in the zy plane of the aligned platinum film immediately after deposition before the lipid template was removed, as shown in Fig. 5a. In this image both a spot pattern and rings are observed, features previously displayed when separately imaging the platinum structures and the lipid films respectively. The peak positions for the spot pattern and those from the rings shown in the radial profile (Fig. 5b) agree with our previous measurements for the platinum nanostructures and phytantriol in excess water: the lattice parameters are found to be a = 67.6 ± 0.5 Å for the lipid and a = 146.4 ± 0.6 Å for the platinum film. The predicted spot patterns for an Fd3m structure aligned with the (111) plane parallel to the substrate have been superimposed onto the image and show good agreement with the measured data. The two rings measured from the lipid again do not show any overall orientation, demonstrating that the aligned platinum structures are being produced from polydomain lipid template.
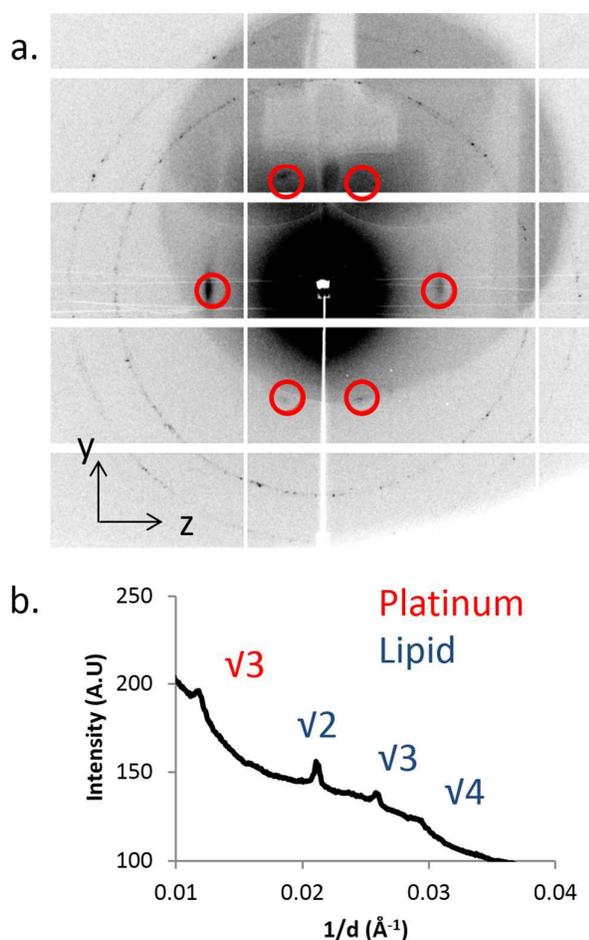
In order to explain this surprising result, we suggest that while overall the lipid is polydomain, the lipid close to the substrate/lipid interface exhibits an overall orientation. Theoretical calculations have shown that for an interface where the Q_{II} lipid bilayer remains continuous and closed, the energy is minimised when parallel to the (111) planes [25,27]. Our grazing-incidence SAXS studies of different spin-coated Q_{II} films between 0.2 and 1 µm thick all confirmed this orientation[27]. Such films have interfaces with a hydrophobic substrate, on one side, and a vapour phase, on the other, either or both of which could induce the observed orientation. In the current work, our results can be explained by the same phenomenon occurring at the lipid/electrode interface.

To test the hypothesis that an orientated region of cubic phase was located close to the lipid/substrate interface we produced films with longer deposition times up to 15 minutes, as compared with the 5 minutes we had used previously. Longer deposition times result in thicker mesoporous platinum films as they grow deeper into the Q_{II} template coating, away from the electrode. Film thicknesses were estimated to be 1.9 ± 0.2 µm (from 5 minutes of deposition), 2.5 ± 0.2 µm, 2.8 ± 0.3 µm and 3.3 ± 0.2 µm as determined by SEM measurements described in S6. Fig. 6 shows 2D images and azimuthal integrations of the scattered ring for films of varying thickness. Predicated azimuthal angles are marked by vertical lines; an offset angle was again added to compensate for the angle between the y axis of the foil samples and the detectors vertical axis. Films of thickness up to 2.8 ± 0.3 µm were observed to display orientation of the (111) parallel to the substrate. The 3.3 µm film was found to be more disordered with no defined orientation. Interestingly a film measured to be 2.5 ± 0.2 µm thickness was observed to feature the (110) orientation in addition to the (111) orientation; in earlier GISAXS work, lipid films produced by allowing a drop of lipid solution in chloroform to run down an angled substrate displayed both the (111) and (110) orientations; such films were less uniform, and likely to have thicker regions[25]. These results are consistent with a Q_{II} lipid template that is overall polydomain and unoriented, but with a region a few microns thick close to the lipid/substrate interface oriented with (111) parallel to the substrate.

Figure 6. (a) SAXS image taken in the zy plane of the platinum nanostructure after deposition and submerged in water before lipid template is removed. (b) Radial profile of the total image with the platinum and lipid peaks Bragg peaks labelled. Limitations in setup resulted in large amount of air scatter which produced a shadow on the top right.

Figure 7. (a) 2D SAXS images of nanostructured platinum films taken in zy plane with varying thickness (a-d) with azimuthal integrations of each image (e-h), (a, e) thickness = 1.9 ± 0.2 µm, (b, f) thickness 2.5 ± 0.2 µm, (c, g) thickness 2.8 ± 0.3 µm, (d, h) thickness = 3.3 ± 0.2 µm. Predicted azimuthal angles for (111) plane orientated parallel to the substrate are shown by dashed lines for e, g and h, predicted angles for (111) and (110) are shown on f by dashed and solid lines respectively.

Conclusions

In conclusion we present a new aligned platinum structure featuring an Fd3m 'single diamond' morphology orientated with the (111) plane parallel to the substrate. Our further data in the presence of the lipid template and with varying film thickness suggests that this alignment arises because the dip coated lipid films, while polydomain on average, adopt a structure within a few microns of the substrate which is uniaxially aligned with the (111) plane orientated parallel to the substrate, consistent with energetic predictions of low-energy Q_{II} interfaces. The orientation of this region is replicated in thinner films of template platinum. These findings give a new insight into the Q_{II}-electrode interface, and have implications for the production of functional nanomaterials.

Acknowledgements

Notes and references

1 J. R. Felts, M. S. Onses, J. A. Rogers and W. P. King, *Adv. Mater.*, 2014, **26**, 2999–3002.
2 X. Zhang, W. Lu, J. Da, H. Wang, D. Zhao and P. A. Webley, *Chem. Commun.*, 2009, 195–197.
3 J. Kibsgaard, Y. Gorlin, Z. Chen and T. F. Jaramillo, *J. Am. Chem. Soc.*, 2012, **134**, 7758–7765.
4 C.-F. Cheng, H.-Y. Hsueh, C.-H. Lai, C.-J. Pan, B.-J. Hwang, C.-C. Hu and R.-M. Ho, *NPG Asia Mater.*, 2015, **7**, e170.
5 V. Mamaeva, J. M. Rosenholm, L. T. Bate-Eya, L. Bergman, E. Peuhu, A. Duchanoy, L. E. Fortelius, S. Landor, D. M. Toivola, M. Linden and C. Sahlgren, *Mol. Ther.*, 2011, **19**, 1538–1546.
6 J. S. Beck, J. C. Vartuli, W. J. Roth, M. E. Leonowicz, C. T. Kresge, K. D. Schmitt, C. T. W. Chu, D. H. Olson and E. W. Sheppard, *J. Am. Chem. Soc.*, 1992, **114**, 10834–10843.
7 Y. Shi, B. Guo, S. A. Corr, Q. Shi, Y.-S. Hu, K. R. Heier, L. Chen, R. Seshadri and G. D. Stucky, *Nano Lett.*, 2009, **9**, 4215–4220.
8 S. A. G. Evans, J. M. Elliott, L. M. Andrews, P. N. Bartlett, P. J. Doyle and G. Denuault, *Anal. Chem.*, 2002, **74**, 1322–1326.
9 U. Bach, D. Lupo, P. Comte, J. E. Moser, F. Weissörtel, J. Salbeck, H. Spreitzer and M. Grätzel, *Nature*, 1998, **395**, 583–585.
10 L. Omer, S. Ruthstein, D. Goldfarb and Y. Talmon, *J. Am. Chem. Soc.*, 2009, **131**, 12466–12473.
11 D. Wang, H. Luo, R. Kou, M. P. Gil, S. Xiao, V. O. Golub, Z. Yang, C. J. Brinker and Y. Lu, *Angew. Chem.*, 2004, **116**, 6295–6299.
12 E. J. W. Crossland, M. Kamperman, M. Nedelcu, C. Ducati, U. Wiesner, D.-M. Smilgies, G. E. S. Toombes, M. A. Hillmyer, S. Ludwigs, U. Steiner and H. J. Snaith, *Nano Lett.*, 2009, **9**, 2807–2812.
13 H. Wang, H. Y. Jeong, M. Imura, L. Wang, L. Radhakrishnan, N. Fujita, T. Castle, O. Terasaki and Y. Yamauchi, *J. Am. Chem. Soc.*, 2011, **133**, 14526–14529.
14 V. N. Urade, T. C. Wei, M. P. Tate, J. D. Kowalski and H. W. Hillhouse, *Chem. Mater.*, 2007, **19**, 768–777.
15 M. R. J. Scherer, P. M. S. Cunha and U. Steiner, *Adv. Mater.*, 2014, **26**, 2403–7.
16 G. S. Attard, J. M. Corker, C. G. Göltner, S. Henke and R. H. Templer, *Angew. Chemie Int. Ed. English*, 1997, **36**, 1315–1317.
17 G. S. Attard, *Science*, 1997, **278**, 838–840.
18 S. Akbar, J. M. Elliott, M. Rittman and A. M. Squires, *Adv. Mater.*, 2013, **25**, 1160–1164.
19 J. Barauskas and T. Landh, *Langmuir*, 2003, **19**, 9562–9565.
20 T. Oka and H. Hojo, *Langmuir*, 2014, **30**, 8253–8257.
21 J. S. Biggins, M. Warner and K. Bhattacharya, *Phys. Rev. Lett.*, 2009, **103**, 037802.
22 N. Yamashita, S. Watanabe, K. Nagai, M. Komura, T. Iyoda, K. Aida, Y. Tada and H. Yoshida, *J. Mater. Chem. C*, 2015, **3**, 2837–2847.
23 S. Vignolini, N. A. Yufa, P. S. Cunha, S. Guldin, I. Rushkin, M. Stefik, K. Hur, U. Wiesner, J. J. Baumberg and U. Steiner, *Adv. Mater.*, 2012, **24**, OP23–OP27.
24 J. A. Dolan, B. D. Wilts, S. Vignolini, J. J. Baumberg, U. Steiner and T. D. Wilkinson, *Adv. Opt. Mater.*, 2015, **3**, 12–32.

25 M. Rittman, H. Amenitsch, M. Rappolt, B. Sartori, B. M. D. O'Driscoll and A. M. Squires, *Langmuir*, 2013, **29**, 9874–9880.

26 L. Latypova, W. T. Góźdź and P. Pierański, *Langmuir*, 2014, **30**, 488–495.

27 S. J. Richardson, P. A. Staniec, G. E. Newby, N. J. Terrill, J. M. Elliott, A. M. Squires and W. T. Góźdź, *Langmuir*, 2014, **30**, 13510–13515.

28 A. M. Seddon, G. Lotze, T. S. Plivelic and A. M. Squires, *J. Am. Chem. Soc.*, 2011, **133**, 13860–13863.

29 A. M. Squires, J. E. Hallett, C. M. Beddoes, T. S. Plivelic and A. M. Seddon, *Langmuir*, 2013, **29**, 1726–1731.

30 A. M. Seddon, J. Hallett, C. Beddoes, T. S. Plivelic and A. M. Squires, *Langmuir*, 2014, **30**, 5705–5710.

31 T. Paik, D.-K. Ko, T. R. Gordon, V. Doan-Nguyen and C. B. Murray, *ACS Nano*, 2011, **5**, 8322–8330.

32 S. J. Richardson, P. A. Staniec, G. E. Newby, J. L. Rawle, A. R. Slaughter, N. J. Terrill, J. M. Elliott and A. M. Squires, *Chem. Commun.*, 2015.

33 M. Rittman, M. Frischherz, F. Burgmann, P. G. Hartley and A. Squires, *Soft Matter*, 2010, **6**, 4058–4061.

34 R. Bilewicz, P. Rowiński and E. Rogalska, *Bioelectrochemistry*, 2005, **66**, 3–8.

35 S. Akbar, PhD Thesis, University of Reading, 2012.

36 S. L. Gras and A. M. Squires, *Methods Mol. Biol. Clifton NJ*, 2011, **752**, 147–163.

37 T. Snow, M. Rittman and A. Squires, *YAX*, cunninglemon.com 2014.

38 P. M. De Wolff, *J. Polym. Sci.*, 1962, **60**, S34–S36.